Pergamon

Journal of Structural Geology, Vol. 17, No. 2, pp. 245 to 256, 1995

0191-8141/95 $9.50+0.00

0191-8141(94)E0039-2

Palaeostress superimposition deduced from mesoscale structures in limestone: the Matelles exposure, Languedoc, France

J.-P. PETIT and M. MATTAUER

Laboratoire de Géophysique et Tectonique et U.R.A. C.N.R.S., Université Montpellier II, Place E. Bataillon, 34095 Montpellier, Cédex 5, France

(*Received* 4 *December* 1991; *accepted in revised form* 10 *March* 1994)

Abstract—This study investigates the reasons for the superimposition of several maximum principal stress directions (σ_1) in the same area, and examines the contrast between unperturbed areas (stable direction of σ_1) and perturbed areas (changing σ_1 direction). We studied mesoscale structures on a 1000 m^2 continuous limestone exposure near a regional scale strike-slip fault. Local σ_1 directions were deduced from a high concentration of minor strike-slip faults, extension fractures and stylolites formed during the Pyrenean shortening in Languedoc, France. Most of the stylolites were formed in a stress field which was homogeneous on the exposure scale. This was followed by the reactivation of pre-existing extension fractures as strike-slip faults whose activity determined stress perturbations. A very heterogeneous stress field was produced leading to the formation of new localized stylolites and extension fractures, especially at fault terminations and at oversteps. Thus the final pattern shows the superimposition of all these structures. Reactivation of structures was caused by slight temporal changes in the orientation and intensity of the stress field produced by the nearby regional strike-slip faults. Our study suggests that the origin of stress deviations or superimpositions cannot be explained by random measurements of σ_1. It is essential to be able to synthesize the fault pattern and the stress trajectories which it determines, and to do this, a very high density or a selection of data from mesoscale structures is needed.

INTRODUCTION

The Jurassic limestones in the Pyrenean foreland of the Languedoc region (Fig. 1) exhibit a high density of mesoscale structures, mainly stylolites and associated extension fractures (Arthaud & Mattauer 1969a) which are related to the Pyrenean shortening (40 Ma) (Arthaud & Mattauer 1969b). These features, found on scattered exposures, enable the local stress orientations to be determined, and hence regional shortening or stress trajectories can be interpreted (Arthaud & Choukroune 1972, Rispoli 1978, Mattauer & Mercier 1984, Ritz 1991). Some unpublished theses have been devoted to the description and interpretation of mesoscale structures for particular exposures in the region (e.g. Liu 1983, Taha 1986). These studies either show that the main compressive stress trajectory trends N20° with only small spatial fluctuations over large areas of several square kilometers, or is very variable from one place to another with superimpositions of several directions in the same place (Fig. 2). Variations in the stress trajec-

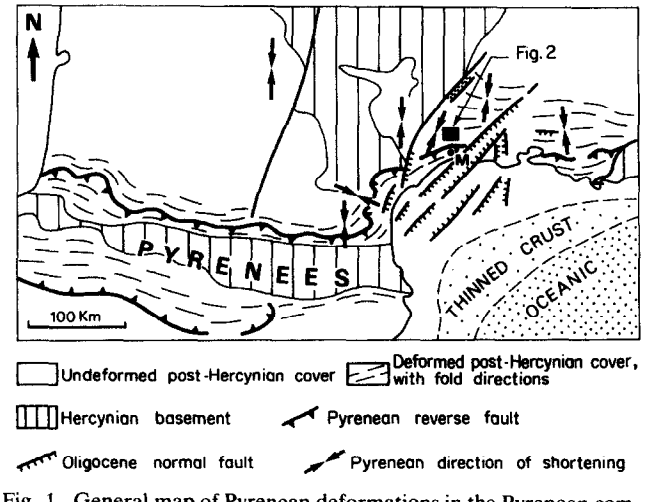

Fig. 1. General map of Pyrenean deformations in the Pyrenean compressive foreland with some shortening directions. M = Montpellier. Position of Fig. 2 shown.

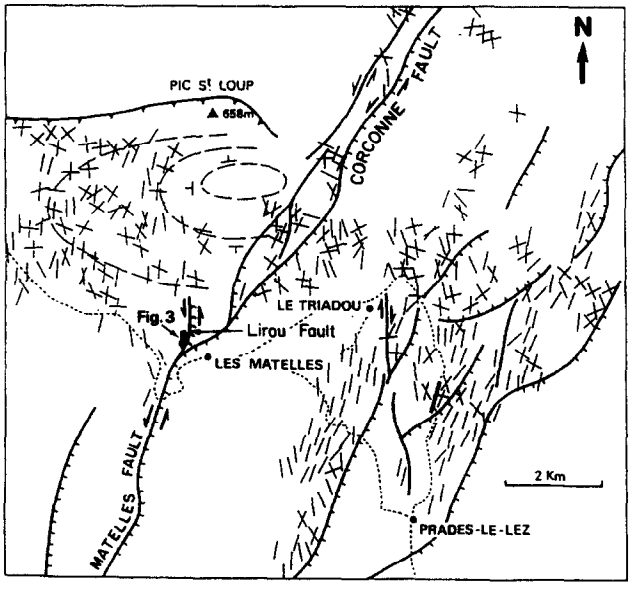

Fig. 2. Map of the area north of Montpellier (see Fig. 1), showing main faults (reverse shown by barbs, strike-slip by arrows and normal by perpendicular dashes). The local Pyrenean main compressive stress orientations given by line segments, are deduced from mesoscale structures (from Taha 1986). Location of measurements is at the middle of the line segments. Crossing line segments indicate the coexistence of two different directions of compression. Dashed lines indicate the traces of layers around the Pic St. Loup Anticline. Location of Fig. 3 shown.

tory can be explained by observations of mesoscale structures: for example, stress trajectories deviating adjacent to minor faults (Delair 1977, Liu 1983), or larger-scale anticlockwise deviations near the major left lateral Cévennes Fault (Mattauer & Mercier 1984). We will present a case study showing the coexistence of simply organized areas, which indicate a rather stable and homogeneous paleostress state, with complex areas having superimposed deformations. The significance of such superimposition is poorly understood and seldom discussed in structural geology, in spite of the importance of such zones for geotechnical, seismotectonic or hydrological problems.

The main reason why this problem remains unsolved is that the studied exposures or areas are usually discontinuous, so that the transitions from simple to complex zones cannot be observed. This study deals with a hectometric-scale exposure where a very high density of mesoscale structures can be continuously observed across almost the entire area. In addition, this exposure is situated in the vicinity of the regional scale Matelles Fault, whose polyphase activity is well know (1/50000 Geological map of Montpellier).

This exposure has been partly described by Rispoli (1981) who analyzed the fault-extension fractures and stylolite features in a brittle kink-band, which implies stress/strain deviation and concentration at the tip of a reactivated fracture. These features led to a model of a small fault, which largely inspired Fletcher & Pollard's (1981) anticrack model for pressure solution surfaces, and provided an illustration of theoretical models of displacements and stresses at faults (Pollard & Segall 1987). However, the features described by Rispoli (1981) dealt with two very local features at the scale of a few dm^2 and were not related to the other features of the exposure. Here we present the entire deformation and the variations of the corresponding stress field over an exposure of more than 1000 m^2.

TECTONIC SETTING

The Matelles exposure (Fig. 3) is situated on one branch of the Matelles Fault, called the Lirou Fault (Figs. 2 and 3). The Matelles Fault can be followed continuously for 20 km to the north-northeast (Corconne Fault) and for 10 km to the south-southeast. Like most of the N20°–30° trending faults north of Montpellier, this fault had both a Pyrenean left-lateral strike-slip movement of upper Eocene age related to the Pyrenean shortening (40 Ma), and also an Oligocene dip-slip displacement (30 Ma) related to extension in Languedoc (Roure *et al.* 1992). Next to the exposure, on the Lirou Fault, these successive contractional and extensional movements are shown by the presence of gently and steeply pitching slickenside lineations. Extension of Cretaceous age (Blès *et al.* 1989) is not well documented in the Matelles area. The exposure is situated next to a slight clockwise bend of the Matelles Fault which would have been a 'restraining bend' (Sibson 1986) during the Pyrenean left lateral movement.

The exposure provides an enormous amount of data because it occurs along a small flat-bottomed valley, where such small structures as stylolites, narrow extension fractures (isolated and en échelon) and pull-aparts can be clearly observed. The southern part of the outcrop is in contact with the Lirou Fault and the northern part is about 50 m from it. The density of mesoscale structures strongly diminishes to the north beyond the zone represented on Fig. 3. The features are observed in a few very gently (<10°) tilted Jurassic micritic limestone strata 20–30 cm thick. Individual stylolite seams and extension fractures are perpendicular to bedding and limited to the thickness of each bed. Thus their formation occurred in plane strain conditions in each bed. In contrast, faults can be observed cutting through all the beds.

MESOSCALE STRUCTURE DATA

The main problem was to make a survey of the whole length of the exposure showing centimetric to millimetric scale structures. This was solved by a photomosaic on the scale of 1:30, produced using a camera hanging at the tip of a pole 4 m above the surface. Most of the mesoscale structures were traced from the photographs, with information from the exposure being mapped onto the mosaic.

Fault pattern

Mapped faults are limited to the zone described on Figs. 3 and 4(b), with no more faults observed more than 100 m from the exposure northwards from the Lirou Fault. The pattern consists of two conjugate sets of faults. A N20° ± 10°-striking left-lateral set (referred to here as N20°) shows several metre-long straight segments infilled with deformed and striated calcite up to 5 cm thick, numerous contractional (Fig. 4d; and c & d in Fig. 3) or extensional (Figs. 3a & f) jogs, and frequent zones with branching features (Fig. 4a; and b, d & g in Fig. 3). The maximum throw is about 60 cm on one branch, but is generally less. A N140° ± 10° striking right-lateral set (referred to here as N140°) shows the same type of calcite infilling as the N20° set. Individual segments are oblique to the mean axis of the exposure and are widely spaced. No oversteps between these faults are visible. Throws are smaller than on the N20° left lateral faults.

Fig. 3. Detailed map of mesoscale structures on the Matelles exposure, with the situation of other figures. Letters refer to zones cited in the text. Simplified from a photo mosaic.

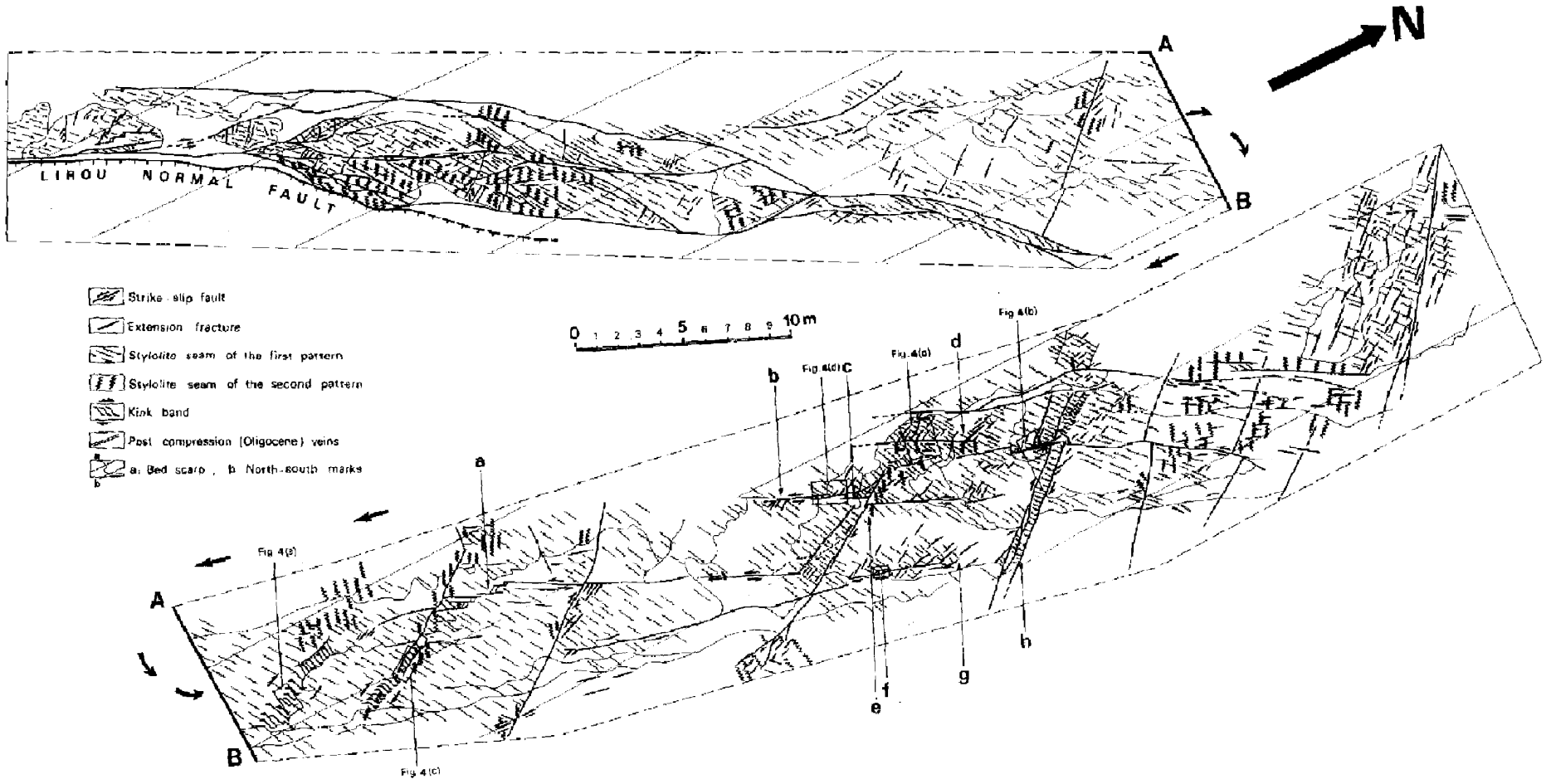
N
A
B
LIROU NORMAL FAULT
Strike - slip fault
Extension fracture
Stylolite seam of the first pattern
Stylolite seam of the second pattern
Kink band
Post compression (Oligocene) veins
a: Bed scarp , b: North-south marks
0 1 2 3 4 5 6 7 8 9 10m
Fig 4(b)
Fig 4(d)
Fig 4(a)
Fig 4(c)
a
b
c
d
e
f
g
h

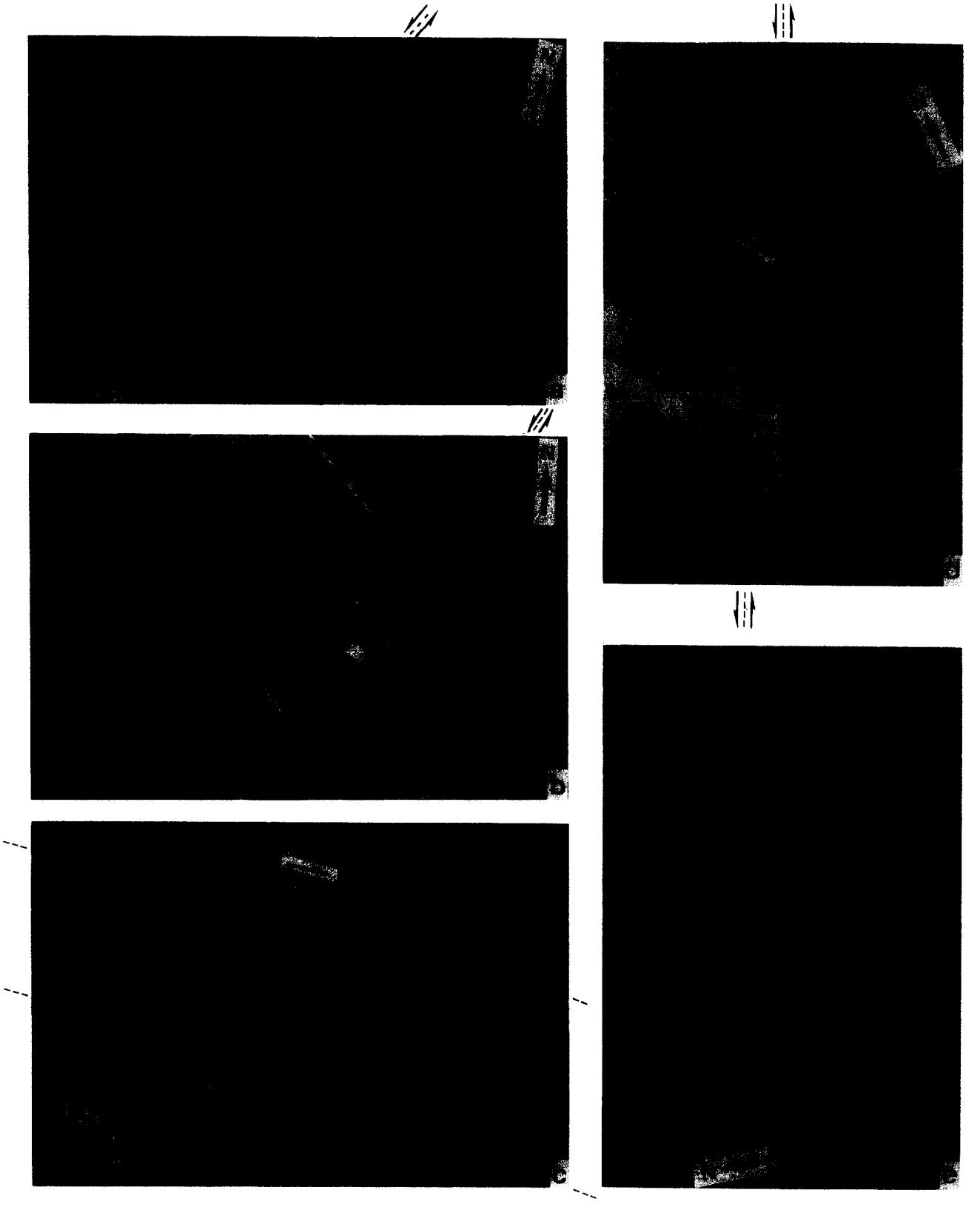

Fig. 4. Features formed during the last deformation episode. (a) Asymmetric deformation linked to the left lateral movement of N30° faults (see Fig. 9 for interpretation); note the N60° stylolites on the left side of the fault and the N100° ones on the right side (outlined by dashed lines). (b) A similar situation as in (a) (along a N15° fault), but with stronger asymmetry and no clear stylolite reorientation on the east. (c) Strongly deformed right lateral kink band (striking N145°) formed by the reactivation of N70° stylolite of the previous episode. (d) Contractional jog between two overstepping N25° fault segments; note the presence of closely-spaced N120° stylolites within the jog zone contrasting with the more widely spaced N55°–60° ones corresponding to the previous episode. (e) Isolated segments (N75°) of stylolites of the first generation reactivated as left lateral strike-slip faults during the formation of a right-lateral kink band with only little movement. Note the extension fracture-stylolite association at the end of these segments. Scales: hammer head 17 cm; pencil 15 cm; knife blade 11 cm.

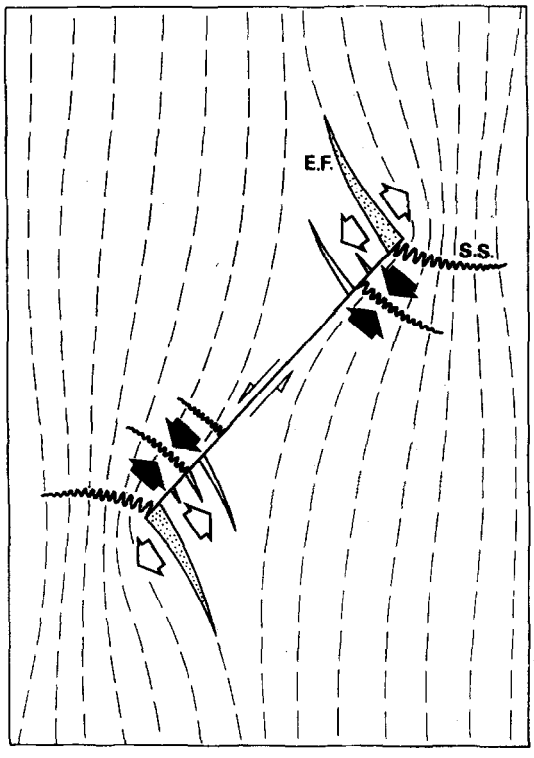

Fig. 5. Idealized sketch of a small fault represented as a vertically loaded mode II crack. The extension fractures (E. F.) propagate from the fault tips along the local σ_1 trajectories in the zone of the strongest perpendicular traction ($\sigma_3 < 0$, white arrows). Stylolite seams (S. S.) formed perpendicular to the σ_1 trajectories (with σ_1 parallel peaks) in the zone of the strongest compression (black arrows).

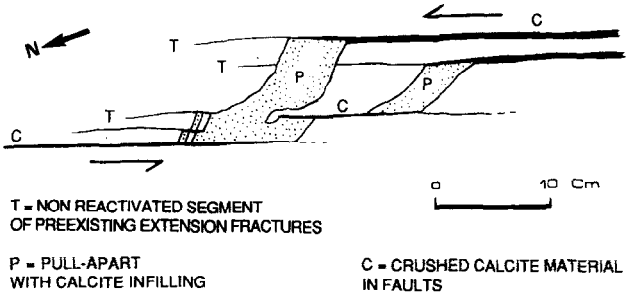

Fig. 6. Pull-aparts on a N20° fault (f on Fig. 3) with non-reactivated segments of the pre-existing extension fractures.

Intersections between the two sets sometimes show that some N20° faults displace N140° ones (e.g. north of Fig. 3), but a high concentration of stylolites at some intersections suggests simultaneous (conjugate) movements on both sets (e in Fig. 3).

Pattern of stylolitic seams and associated extension fractures

Two different sets of planar stylolitic seams are present, both with peaks typically perpendicular to the seam surface. A regular set occurs throughout the exposure. This set corresponds with the locally kinked 'pre-tectonic joint' system described by Rispoli (1981). The dominant direction is N55°–60°, but locally it can be N40° (next to the Lirou Fault), or N70° (towards the north). It will be referred to here as N55°–60°. Locally the direction is constant, and the lateral variations are gradual. Spacing varies from several centimeters to a few millimeters and is quite regular except in a few areas such as in a narrow band between parallel N140° faults (h in Fig. 3). This set is typically nearly orthogonal both to the N140° faults and to N140° striking extension fractures in the northern part of the exposure. Next to some N20° faults, N55°–60° stylolites appear more developed and closely-spaced, and are associated with wide extension fractures which are often cut by the stylolites (Fig. 4a). This set can be observed up to 100 m beyond the northern limit of the exposure, but it becomes less closely-spaced and rapidly vanishes.

A N100° (±10°) set (referred to here as N100°) which is always superimposed on the N55°–60° set can only be observed locally. In the northern part of the exposure stylolites occur in contractional jogs along the N20° faults (Fig. 4d; d in Fig. 3) or in damping zones (Granier 1985) (Fig. 4a). These features suggest a genetic link between this set and the N20° faults. This N100° pattern is also occasionally linked to the N140° faults (centre of Fig. 3). It is more widespread in the immediate vicinity of the Lirou Fault and appears in areas more or less approximately bounded by N20° minor faults.

Kink bands

One of the most remarkable features of this exposure, seldom found elsewhere in the region, are right-lateral kink bands formed by the local rotation (by about 10°) of the N55°–60° stylolitic seams (e.g. centre of Figs. 3 and 4c). They were described by Rispoli (1981) who considered the stylolites to be pre-tectonic joints. The individual rotated stylolites segments were reactivated as small faults with left-lateral antithetic movement accommodating rotation within the right-lateral kink. This geometry can be compared with that of joint drags (Dewey 1966), but here, the ends of small faults show particular extension fractures and stylolite associations (Fig. 4e). These individual features have been taken as models of small faults (see references below) as they show the features associated with the shear movement on a limited pre-existing defect in mode II conditions (Fig. 5). They illustrate the effects of the local stress field at the fault tip, as inferred from experiments (Petit & Barquins 1988) and described from analytical models of the elastic stress field around defects (Anderson 1951, Chinnery 1966, Petit & Barquins 1990, Barquins & Petit 1992) or as an illustration of fracture mechanics predictions (Pollard & Segall 1987). The rotation of the activated segments can be pronounced, leading to complex extension fractures and stylolite associations within a band whose edges form a continuous rupture zone (Fig. 4c). The kink bands are right-lateral, and trend N140° and N170° (Fig. 3). A few kink bands with a N170° trend can also be observed beyond the northern limit of the mapped area. In all cases the band axes are nearly perpendicular to the N55°–60° seams set. Locally, kinks can be seen along the N140° faults (continuation of Fig. 4c on Fig. 3).

Sinuous extension fractures

Sinuous isolated extension fractures with coarse-grained iron-oxide-rich calcite infilling up to 10 cm thick are present in several places over the exposure. In spite of their N20°–30° mean trend, they cannot be confused with any of the above structures. They are probably linked to the Oligocene extension, so they will not be taken into account in the discussion of the effects of the Pyrenean shortening.

ANALYSIS AND MECHANICAL INTERPRETATION

Methods and terminology

The analysis is based on classical interpretations of mesoscale features in limestones (e.g. Blacke & Roy 1949, Arthaud & Mattauer 1969a,b, Mattauer 1978). Extension fractures are perpendicular to the local direction of extension and parallel to the shortening which is also indicated by the direction of stylolite peaks. On most of the exposure, peaks are usually perpendicular to the stylolite surfaces, so the latter can be interpreted as anti-cracks (Fletcher & Pollard 1981). Strictly speaking stylolites and extension fractures give the trajectories of the finite shortening axis Z. As in Rispoli (1981) they will be considered as approximate indicators of the stress trajectories of σ_1 (main principal stress) which prevailed during the deformation. This can be justified by the small amount of deformation due to tensile rupture and pressure solution (Gratier 1993) and by the lack of evidence to indicate significant block rotations, either on the exposure (except in kinks), or in the region. Maps of the σ_1 trajectories on most of the exposure can be drawn from the abundant and continuous mesoscale features. They provide evidence for stress deviations: i.e. local orientations of σ_1 with respect to the general (mean) orientation of these trajectories found in the mapped area. This general orientation can be seen as the remote compressive stress axis applied at the limits of the

studied system. The term 'perturbation' indicates both stress deviation indicated by mesoscale structures of a particular orientation, and the corresponding principal stress values indicated by the high density of the mesoscale structures. Such perturbations will be also discussed on a regional scale.

Origin of mesoscale structures

The two superimposed stylolite sets indicate two episodes of pressure solution-related compression localized adjacent to the Lirou strike-slip fault. The first episode corresponds to the N55°–60° set. The influence of the Lirou Fault on this set is shown by a slight change in σ_1 direction, northwest very close to the fault and north-northwest further away. The second episode corresponds to the N100° set. The corresponding local compression (σ_1) varies between N0° and N30° at different locations when deduced from stylolites. The relationship between this set and the left lateral N20° faults particularly at contractional jogs indicates that this compression is related to the fault movements.

Two different ideas about the stress field emerge: are these two superimposed stress fields the result of two different compressive episodes (i.e. with a change in the direction of the remote stress)? Or is the superimposition only a local effect linked to rupture on N20° faults (i.e. with the same direction of the remote stress)? The problem cannot be solved unless a clear scenario for the formation of all the observed structures is established, including their chronology and the corresponding stress states. A key question for the stress orientations is whether the N20° and N140° local strike-slip faults were formed in intact rocks, or if they were reactivated pre-existing fractures. Rispoli (1978) was in favour of the first hypothesis and analysed these faults as conjugate, and formed in intact rock. Thus the most favourable σ_1 direction for their formation would be the acute bisecting angle (N170°), in which case the N100° stylolite set can be explained by the effect of the N20° fault propagation. But in fact, the formation of the N55°–60° pattern is not compatible with this bisecting direction and implies an earlier episode in which σ_1 was oriented at about N145°. If these faults are reactivated pre-existing fractures, the scenario must be based on the chronology for fractures, faults and N55°–60° stylolites formation, which has to be demonstrated from detailed observations.

Several points show that N20° faults are reactivated extension fractures. First, the associated deformation occurs only at oversteps or at fault tips; that is in situations implying local stress concentrations typically associated with reactivated fractures (see detailed interpretation below). Secondly, the fault surfaces are sharp and rectilinear, with no traces of extension fractures or stylolites typically associated with shear rupture in carbonate rocks (Mattauer 1978). Thirdly, numerous faults show lozenge-shaped pull-apart structures (extensional jogs) inherited from pre-existing overlapping extension fractures, as shown by the presence of non-reactivated segments (one to a few mm wide) adjacent to pull-aparts (Fig. 6). For the N140° faults, only the second reason can be given, but their origin as early extension fractures is attested by the presence of such fractures of the same direction outside the exposure. Figure 7, which shows similar directions for the faults in the studied area and for extension fractures in the north of the exposure, provides evidence for the reactivation hypothesis for both fault sets.

Chronology of structures

The association of N140° faults with the nearly orthogonal N55°–60° seam set is striking. As these faults have been interpreted as reactivated extension fractures, it is tempting to conclude that the N140° extension fractures and the N55°–60° stylolite pattern were formed together, with the same σ_1 direction during the same episode. But this association is probably just accidental: the N140° extension fractures commonly found in Languedoc most probably forming during the Cretaceous extension, so clearly preceded the main Pyrenean shortening (N0°–N40°) with which stylolite seams are typically associated (Rispoli 1978, Tourneret 1990, Arthaud personal communication 1992). Moreover, the exposures show a slight but systematic angle of 5°–10° between the stylolite seams and the perpendicular to the N140° fractures, which does not support a cogenetic hypothesis. Thus we conclude that the N55°–60° stylolite set is not linked to the earlier N140° extension fractures.

The age of the N20° extension fractures which preceded the faulting is quite important. We deduce that they were present as sealed (that is mechanically inactive) fractures before the first episode for two reasons. (i) Had they not been present, until later and therefore formed between the first and the second episode, this would imply a N20°σ_1. Such a σ_1 orientation would easily have reactivated the closely-spaced N55°–60° stylolite seams as left lateral faults, but this is not observed. (ii) Detailed outcrop observations show that the N55°–60° individual stylolite seams either vanish next to non-

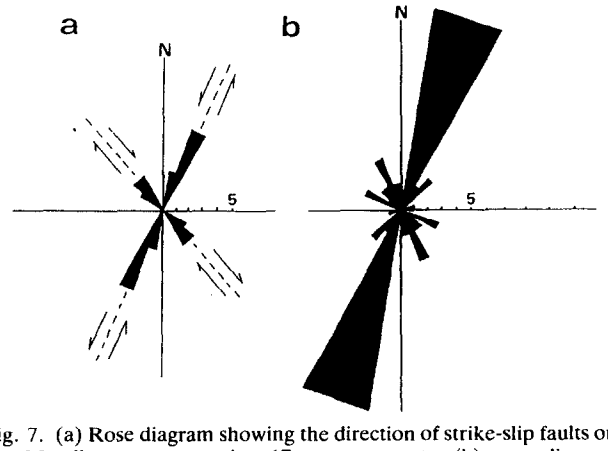

Fig. 7. (a) Rose diagram showing the direction of strike-slip faults on the Matelles exposure using 17 measurements; (b) rose diagram showing the direction of extension fractures, at 100 m north to the exposure, using 40 measurements.

reactivated segments of N20° extension fractures, or offset them.

Thus we conclude that the N55°–60° stylolite set was superimposed onto a pre-existing N20° and N140° extension fracture pattern.

Stress and strain evolution on the exposure scale

Figure 8 summarizes the scenario for the exposure scale stress evolution deduced from the above analysis, excluding the formation of the early N140° extension fractures. The sequence of events is as follows:

(a) A first compressive Pyrenean stage with σ_1 oriented N20° formed the extension fractures without associated stylolite seams (Fig. 8a).

(b) After an anticlockwise rotation of σ_1, a second stage of compression occurred with σ_1 oriented N145°. The accompanying presence of fluids induced the formation of the N55°–60° stylolite seam set by pressure solution within a stress field which was homogenous on the exposure scale (Fig. 8b). At this stage the stress state did not allow extension fracture reactivation

(c) In the third stage, the extension fractures were reactivated as faults with kink formation (Fig. 8c). This probably implies an increase in the differential stress and/or fluid pressure.

This last stage raises the question of whether the reactivation of the two sets of extension fractures is compatible with the same N145° σ_1 as in (b). The problem is that of the best oriented direction of compression for the reactivation of sealed fractures. The reason for the reactivation is that the fractures were sealed with sparitic calcite which is weaker than the surrounding fine grained mudstone. To our knowledge the problem of rupture in such conditions has not been specifically studied in the rock mechanics literature. However, the situation can be compared with that of rupture in anisotropic rocks. Most of the studies deal with one plane of anisotropy (Donath 1964, Masure 1970), and the study of Masure (1970) on two anisotropies (bedding planes and cleavage) cannot be applied because the shear rupture never occurred on both planes during the same experiment. Uniaxial and biaxial tests with one anisotropy show that the ultimate strength diminishes (the rupture occurs at least partly on the corresponding plane) for anisotropy loading axis angles of between about 15° and 50° with a minimum strength from 25° to 40° (Donath 1964). This suggests that the N145° σ_1 which is respectively at 5° and 55° to the extension fractures is not favourable to their reactivation as shear fractures, so that a clockwise rotation of σ_1 towards the bisector (i.e. at N170°) is likely.

Because of tips and overstepping in the N20° extension fractures, the shear reactivation induced a very inhomogeneous (perturbated) local stress field, which was responsible for the formation of the N100° stylolite seams and other associated structures (see below).

The right lateral kink band formation can be discussed on the basis of mechanical models. Most authors agree that non-conjugate contractional kink bands develop when σ_1 is markedly inclined to the anisotropy (see Dewey 1966 and synthesis in Price & Cosgrove 1990). No precise value can be given, but their formation with the same σ_1 as in Fig. 8(b) is excluded, and it implies a late clockwise rotation of σ_1 as in Fig. 8(c). Another interpretation leading to the same conclusion is derived from the fact that three kink band axes are observed

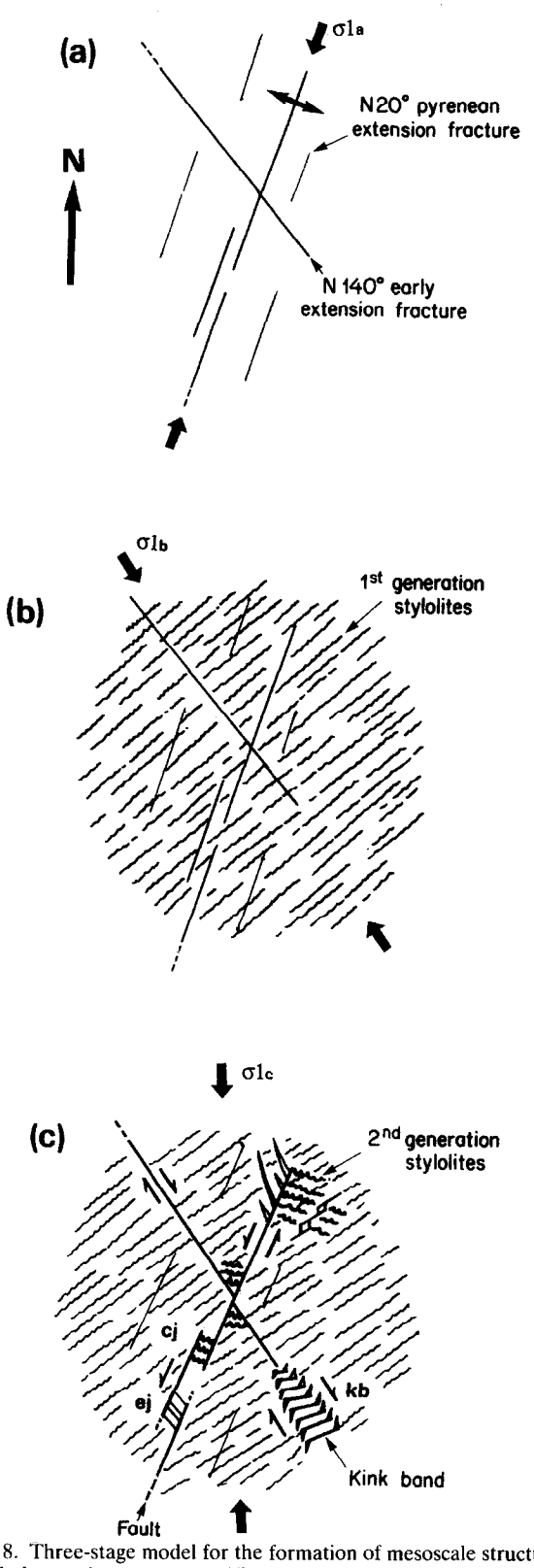

Fig. 8. Three-stage model for the formation of mesoscale structures. Symbols are the same as on Fig. 3; kb = kink band; cj and ej are contractional and extensional jogs, respectively. See text for details.

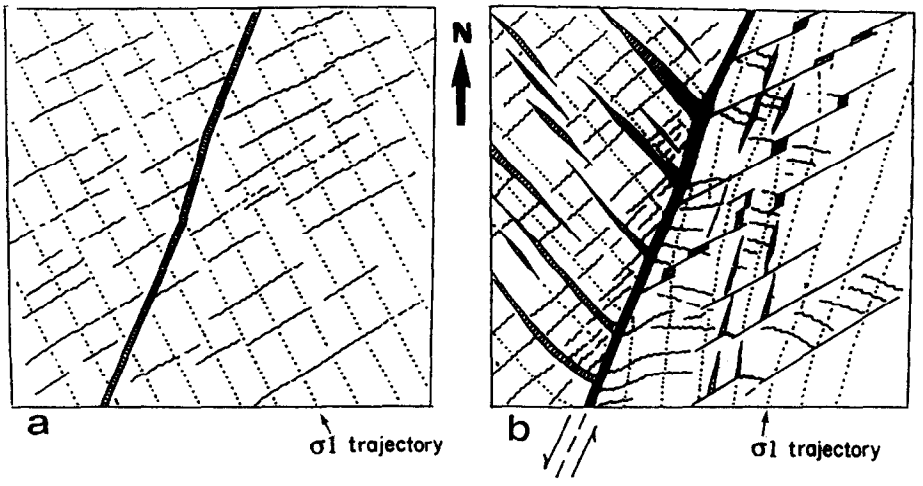

Fig. 9. Sketch of the evolution of stress and strain corresponding to the feature shown on Fig. 4(a) in a N30° fault tip zone. (a) N55°–60° stylolite pattern of the first pressure solution episode and corresponding σ_1 trajectories (dotted lines); the big N30° extension fracture was formed before the stylolites (wavy lines); (b) superimposed structures formed during a later episode which reactivated the extension fracture as a left lateral fault, and corresponding σ_1 trajectories. Striations indicate undeformed calcite infilling of the extension fractures and pull-aparts, while black areas represent crushed and recrystallized calcite in the N30° fault (see text for details).

along the trace of the N140° right lateral faults (northeast of Fig. 4(c), south of Fig. 4(a) and northeast of h in Fig. 3). As shown below, the kinks could correspond to a shear movement at the tips of N140° strike-slip faults. Their formation is thus the consequence of the N140° fault movement, so they formed with the same σ_1 as that needed for extension fracture reactivation.

The N100° stylolite pattern of the southern part of the exposure (next to the Lirou fault) could result from a contractional jog between two N20° faults, with the same N170° σ_1, but it could also imply a more pronounced clockwise reorientation of σ_1 up to N30° at the vicinity of the Lirou Fault.

Mechanical models for the mesoscale structures

Some of the mesoscale structural patterns can be interpreted in detail within the frame of the above scenario. Figure 4(a) shows the asymmetrical features associated with the termination of a N20° fault segment. They have been interpreted by Rispoli (1978) as the result of stress perturbation at the fault tip during its propagation, when σ_1 was oriented N–S. We interpret the deformation as a damping zone (e.g. a zone of high displacement gradient in which the shear displacement vanishes in the fault tip zone, Granier 1985) of the sheared pre-existing fractures. Such situations are often found in non-carbonate rocks where they are characterized by branch fractures of various geometries indicating tensile stress concentrations (Granier 1985, Petit & Barquins 1988, Martel *et al.* 1988). On the Matelles exposure, Rispoli's analysis of individual rotated and sheared segments within the kink bands (as on Fig. 4e) shows that stylolites are concentrated on the side opposite the branched extension fractures at the fault tip, with their peaks tending to become parallel to the fault. This suggests both a reorientation of σ_1 and an increase in its value at the tip. These situations are predicted by experimental and analytical models of an oblique crack in mode II compressive loading conditions (Pollard & Segall 1987, Barquins & Petit 1992). In Fig. 4(a), the N55°–60° stylolite pattern can be recognized on both sides of the fault, unless it is less marked on the east side. This implies a simple stress trajectory pattern during the N145° compression (Fig. 9a). The east side of the zone shows superimposed N100° stylolites and N60° minor faults with pull-aparts at dilatational jogs, which formed by the strike-slip shear fracturing of some stylolite seams of the N55°–60° set. Both N100° stylolites and N60° minor faults indicate a local σ_1 slightly oblique to the fault trace near the tip on the east side (Fig. 9b). The west side shows well marked N55° stylolites, which are superimposed on the stylolites of the N145° compression. They are associated to a particular concentration of thick calcite-infilled extension fractures perpendicular to the stylolites. This association which is not found elsewhere along the fault indicates a northwest local compression. The overall geometry is the result of the superimposition of pre- and syn-slip local stress fields in the fault tip zone. The syn-slip features indicate stress trajectories and concentrations in good agreement with the above analytical models. If such superimpositions were caused by fault tip propagation, they would be present all along the faults, with signs of progressive stress reorientation linked to the propagation of the perturbation; however, this is not observed.

The kink bands can also be interpreted as damping features of the N140° fault (stage c; Fig. 8). Their location can be explained from analytical and experimental models which show that fault propagation in mode II conditions (e.g. perpendicular to the front of a pre-existing defect) can occur either by branching or by a shear deformation zone which extends in front of the fault (sheared defect). In the latter case, the shear deformation is localized in an elongate zone of high differential stress described by analytical models and observed in photoelastic experiments (Petit & Barquins 1988, 1993). These physical models in isotropic

materials show that this shear deformation needs a higher stress level than branching, but here the nearly orthogonal orientation of the N55°–60° stylolite set with respect to the N140° faults probably made the shear deformation easier than branching. The isolated kink band next to the A–B segment on Fig. 3 is not at the tip of a strike-slip fault; it could be the expression of right lateral movements on underlying or overlying faults (propagation by kinking in mode III conditions).

The exposure shows examples of elongated stylolite bands located between parallel faults. In some cases (as in Fig. 4d) a contractional jog geometry indicates that the stylolite was caused by a local compressive stress concentration associated with a deviation during the final compression. In the case of the N140° band (h in Fig. 3), limited by two parallel faults with nearly perpendicular stylolite seams, a contractional jog geometry is not obvious. The stylolite concentration might be caused either by a stress concentration between two reopened extension fractures during the N55°–60° stylolite pattern formation, or by the superimposed deviated stress (guided by the N140° fractures) during the N170° shortening.

Summarizing all these local interpretations enables us to draw up an interpretative map synthesizing the σ_1 stress trajectories during the late episode in the northern part of the exposure (Fig. 10).

Stress and strain evolution of the exposure context

The Lirou Fault (among others) branches off a restraining bend on the Matelles Fault which can be interpreted as a splay strike-slip fault formed during an early stage of the Pyrenean shortening. It is to be noted that the N20° extension fractures formed during the first stage trend, nearly parallel to the Lirou Fault with a decreasing spacing towards it. This could mean that the N20° extension fractures and the incipient Lirou fault may have formed together as extension fractures in a zone of N110° extension east of the Matelles Fault. This effect could be expected from the restraining bend geometry of the Matelles Fault at the beginning of its strike-slip movement. Thus the left-lateral strike-slip movement on the Lirou fault could correspond to the reactivation of a large extension fracture. This hypothesis means that the regional maximum principal stress would have been slightly oblique to the general trend of the Matelles fault at about N0° at the initial stage.

The second stage stress field had σ_1 oriented towards N145°, and controlled the N55°–60° stylolite pattern formation. This implies an anticlockwise rotation of the remote σ_1, or the occurrence of an entirely new stress field. This second stage stress field was unperturbed within the exposure, but the localization of solution surfaces next to the Lirou Fault obviously means that the latter acted as a stress concentrator. Fluids expelled from the Lirou Fault may have facilitated their formation. The stress state on the Lirou Fault could be a local effect of a more general stress concentration due to the restraining bend geometry of Les Matelles fault. The

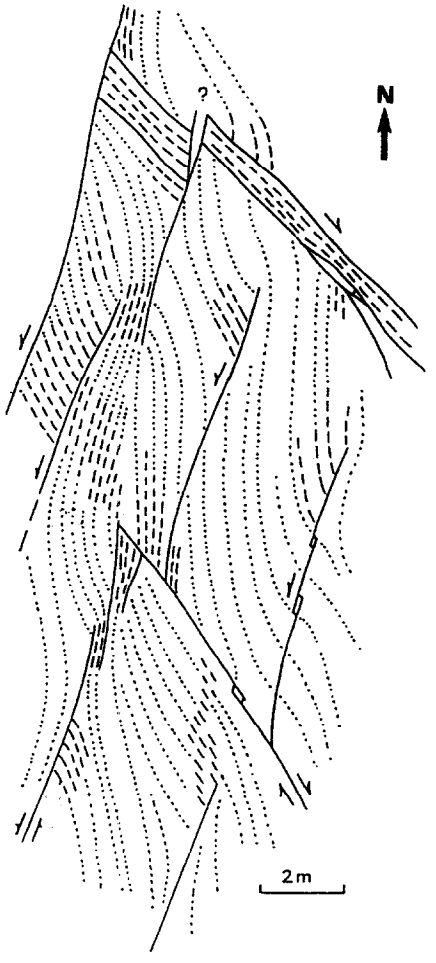

Fig. 10. Interpretative sketch of the second episode σ_1 trajectories over the northern part of the exposure. Unbroken lines = faults; dashed lines = σ_1 trajectories deduced from mesoscale structures; dotted lines = σ_1 trajectories inferred from elastic models indicating parallel and perpendicular tendency of stress trajectories at fault tips (see text for details).

transition to the third stress field on the exposure scale apparently implies both a clockwise rotation and a change in the differential stress magnitudes (increase in σ_1 or decrease in σ_3 values, or both) leading to rupture on pre-existing planes of weakness. As pressure solution was still active, there is no reason to infer a long time gap with the previous stage. This stress evolution could be due to discontinuous slip on the Lirou or Matelles Faults. A seismic rupture between the two stages could have led to such a stress change.

CONCLUSION

This study demonstrates the need for detailed and continuous observations of mesoscale structures for any discussion of palaeostress evolution on a complex exposure. If the metric scale structures alone (such as faults) had been investigated, only one compressive episode would have been recognized. More detailed conclusions required continuous mapping of centimetric to decimetric scale structures such as stylolites, extension fractures and kink bands, and a study of their relationships with the faults and the possible influence of

pre-existing fractures. This approach, with the help of mechanical models, is essential to reveal the reactivation of pre-existing fractures and identify the three stages of deformation of the Matelles exposure. On a larger scale, this study also illustrates how a restraining bend geometry on a fault could generate successive local stress fields, whose superimposition leads to very complex local mesoscale structure patterns.

This study contributes to ideas about regional scale palaeostress trajectories (or directions) in carbonaceous rocks. Most studies are based on extrapolations from local observations of mesoscale structures over sometimes very scattered or small exposures (typically a few m^2), and they do not take into account the possible influence of relatively small faults which are generally not mapped. The regional stress trajectories or local directions are then interpreted as having unexplained, sometimes very strong, fluctuations. This can lead to a rather vague evaluation of the regional stress field orientation, but it cannot explain the stress evolution in space and time, i.e. in terms of stress deviations and superimpositions, respectively. The Matelles analysis demonstrates that an isolated direction does not necessarily represent the mean stress field over the entire zone. A local structure can be formed under the influence of deviations of various scales, generated by faults of various size.

The type of deviations seen on the Matelles exposure may exist elsewhere at larger scales. Therefore if one aims to describe and understand stress trajectories on a regional scale, plotting all the data on mesoscale structures, without the faults, gives a map with limited meaning. Ideally the stress trajectories should be related to the complete fault pattern from the regional scale to metre or decameter scale, as in this example. This is often not realistic. However, it may be possible to obtain significant stress trajectory maps on a regional scale, when a very high density of measurements can be made and when measurements are selected such that local directions related to small faults (i.e. on a scale which prevents them from being represented) may not be taken into account. This implies a special effort to observe the faults in and around the exposure where the local direction is considered. Then the trajectories are drawn from the selected local directions plotted on a map with a very detailed fault pattern.

Acknowledgements—Our grateful acknowledgements to D. C. P. Peacock for his helpful remarks and careful reviewing, and to J. Garcia for the drawings, especially for Fig. 3.

REFERENCES

Anderson, E. M. 1951. *The Dynamics of Faulting*. Oliver and Boyd, Edinburgh.

Arthaud, F. & Choukroune, P. 1972. Méthode d'analyse de la tectonique cassante à l'aide des microstructures dans les zones peu déformées: Exemple de la plateforme Nord-Aquitaine. *Revue de l'Institut due Pétrole* **XXVII**(5), 715–732.

Arthaud, F. & Mattauer, M. 1969a. Exemples de stylolites d'origine tectonique dans le Languedoc, leurs relations avec la tectonique cassante. *Bull. Soc. Géol. Fr.* 7 *Ser.* **XI**, 738–744.

Arthaud, F. & Mattauer, M. 1969b. Sur les décrochements sénestres contemporains des plis pyrénéens du Languedoc. *C. R. Soc. Géol. Fr.* **8**, 290–291.

Blacke, D. B. & Roy, J. C. 1978. Unusual stylolites. *Am. J. Sci.* **247**, 779–790

Blès, J. L., Bonijoly, D., Castaing, C. & Gros, Y. 1989. Successive post-Variscan stress fields in the French Massif central and its borders (Western European plate): Comparison with geodynamic data. *Tectonophysics* **169**, 79–111.

Carte géologique de Montpellier au 1/50000 Service Géologique National.

Chinnery, M. A. 1966. Secondary faulting. I. Theoretical aspect. *Can J. Earth Sci.* **3**, 163–190.

Delair, J. 1977. Fracturation des roches calcaires, Tome 2: Etude détaillée des microstructures cassantes et des stylolites affectant un calcaire micritique: analyse géométrique et cinématique, essai d'interpretation génétique. Thèse 3° Cycle, Montpellier.

Dewey, J. F. 1966. Kink-bands in Lower Carboniferous slates of Rush, Co. Dublin. *Geol. Mag.* **103**, 138–142.

Donath, F. A. 1964. Strength variations and deformational behaviour in anistropic rock. In: *State of Stress in the Earth Crust* (edited by Judd. W. R.). Int. Conf. June 1963, Santa Maria, Elsevier, New York, 281–298.

Fletcher, R. C. & Pollard, D. D. 1981. Anticrack model for pressure solution surfaces. *Geology* **9**, 419–424.

Granier, T. 1985. Origin, damping and pattern of development of faults in granite. *Tectonics* **4**, 721–737.

Gratier, J. P. 1993. Le fluage des roches par dissolution-cristallisation sous contrainte dans la croûte supérieure. *Bull. Soc. Géol. Fr.* **2**, 267–288.

Liu, X. 1983. Perturbations de contraintes liées aux structures cassantes dans les calcaires fins due Languedoc. Observations et simulations mathématiques. Thèse 3ème Cycle, Montpellier.

Martel, S. J., Pollard, D. D. & Segall, P. 1988. Development of simple strike-slip fault zones, Mount Abbot Quadrangle, Sierra Nevada, California. *Bull. Geol. Soc. Am.* **100**, 1451–1465.

Masure, P. 1970. Comportement des roches à anisotropie planaire discontinue, application à l'étude de la stabilité des excavations souterraines. Thèse d'Etat, Sc. Appl. Nancy No AO 4202.

Mattauer, M. 1978. Les déformations des matériaux de l'écorce terrestre. Hermann édit. Paris.

Mattauer, M. & Mercier, J. L. 1984. Microtectonique et grande tectonique. Spec. issue of the *Bull. Soc. Géol. Fr.* **10**, 141–161.

Petit, J.-P. & Barquins, M. 1988. Can natural faults propagate under Mode II conditions? *Tectonics* **7**, 1243–1256.

Petit, J.-P. & Barquins, M. 1993. Localisation des bandes de cisaillement par un défaut isolé préexistant: données experimentales. *Bull. Soc. Géol. Fr.* **2**, 255–266.

Pollard, D. D. & Segall, P. 1987. Theoretical displacements and stress near fractures in rocks: with applications to faults, joints, veins, dikes, and solution surfaces. In: *Fracture Mechanics of Rock* (edited by Atkinson B. K.). Academic Press, London, 277–349.

Price, N. J. & Cosgrove, J. W. 1990. *Analysis of Geological Structures*. Cambridge University Press, Cambridge.

Rispoli, R. 1978. Microtectoniques et champ de contraintes dans les calcaires fins du Languedoc. Exemples des Matelles et du Cirque de Navacelles. Thèse 3ème Cycle, Montpellier.

Rispoli, R. 1981. Stress field about strike-slip faults inferred from stylolites and extension fractures. *Tectonophysics* **75**, T29–T36.

Ritz, F. 1991. Evolution du champ de contrainte dans les Alpes du sud depuis la fin de l'Oligocène. Implications sismotectoniques. Thèse Montpellier.

Roure, F., Brun, J. P., Coletta, B. & Van Den Driessche, J. 1992. Geometry and kinematics of extensional structures in the Alpine Foreland Basin of southern France. *J. Struct. Geol.* **14**, 503–519.

Sibson, R. H. 1990. Conditions for fault valve behaviour. In: *Deformation Mechanisms, Rheology and Tectonics. Spec. Publs geol. Soc. Lond.* **54**, 15–28.

Taha, M. 1986. Apport de la microtectonique cassante au problème des trajectoires de contraintes et de leurs perturbations. Exemples du nord de Montpellier. Thèse d'Etat, Montpellier.

Tourneret, C. 1990. Maclage et état de contrainte dans les roches carbonatées du domaine fragile. Applications à des plateformes d'avant-pays de chaines (Pyrénées, Alpes). Thèse de Doctorat, Montpellier.